

See discussions, stats, and author profiles for this publication at: <https://www.researchgate.net/publication/40193273>

Long Minority Chains in a Polymer Brush: A First-Order Adsorption Transition

ARTICLE in *MACROMOLECULES* · MARCH 1999

Impact Factor: 5.8 · DOI: 10.1021/ma981401q · Source: OAI

CITATIONS

25

READS

20

4 AUTHORS:



[Alexander M. Skvortsov](#)

Chemical Pharmaceutical Academie . St.Pete...

151 PUBLICATIONS **1,680** CITATIONS

[SEE PROFILE](#)



[Alexei A. Gorbunov](#)

Institute for Highly Pure Biopreparations, Sai...

90 PUBLICATIONS **1,506** CITATIONS

[SEE PROFILE](#)



[Frans A M Leermakers](#)

Wageningen University

289 PUBLICATIONS **4,755** CITATIONS

[SEE PROFILE](#)



[Gerard J Fleer](#)

Wageningen University

205 PUBLICATIONS **8,376** CITATIONS

[SEE PROFILE](#)

Long Minority Chains in a Polymer Brush: A First-Order Adsorption Transition

A. M. Skvortsov

Chemical-Pharmaceutical Academy, Prof. Popova 14, 197022 St. Petersburg, Russia

A. A. Gorbunov

*State Research Institute for Highly Pure Biopreparations,
7 Pudozhskaya, 197110 St. Petersburg, Russia*

F. A. M. Leermakers and G. J. Fleer*

*Laboratory of Physical Chemistry and Colloid Science, Wageningen Agricultural University,
Dreijenplein 6, 6703 HB Wageningen, The Netherlands*

Received September 3, 1998; Revised Manuscript Received December 28, 1998

ABSTRACT: We discuss polymer brushes containing a small fraction of minority chains that differ from the majority brush-forming chains both in length and in chemical structure. We consider the situation that the solvent is good for both types of chain. Furthermore, we assume that the minority chains are longer than the brush chains and consist of adsorption-active monomers, which therefore are able to adsorb onto grafting surface. We examine this case by numerical self-consistent-field calculations for a lattice model and by an analytical continuum theory. The contour length and the adsorption interaction parameter of the minority chains are the variables. With the numerical model, we show that the minority chains undergo a cooperative transition from an adsorbed state to a flower conformation consisting of a stretched stem and a coiled crown. The end-point distribution for the minority chains turns out to be bimodal. The analytical theory, using a two-state approximation, describes the conformational adsorbed chain-to-flower transition as a first-order phase transition (in the appropriate thermodynamic limit). The dependence of the transition point on the chain length ratio, the grafting density of the brush chains, and the adsorption energy of the minority chains is analyzed in some detail. The influence of a depletion zone near the grafting surface in a brush on the transition point is discussed.

1. Introduction

Polymer chains attached by one end to a surface or a liquid–liquid interface with a high enough anchoring density form a brush. Polymer brushes are of substantial technological importance for example in surface modification, stabilization and flocculation of colloidal dispersions, etc. Therefore, brushes have been extensively investigated, both experimentally and theoretically.^{1–4} So far, most analytical results were obtained for regular brushes formed by monodisperse homopolymer molecules in a good solvent. The brush structure in equilibrium is now understood rather well. Self-consistent-field (SCF) theories provide a basic analytical description and are widely used in interpreting experimental data.^{5,6}

However, several interesting (and strong) effects are precisely due to an inhomogeneity in the brush composition. We argued earlier^{7,8} that a minority chain A, added to a homogeneous monodisperse brush on a flat surface and differing from the majority brush-forming chains B in length N , may take three different types of conformation, depending on the lengths of N_A and N_B of A and B chains, respectively [we use the subscript A for the added (adsorbing) minority chains, and the subscript B for the majority brush chains; the thickness of a pure brush B is denoted as H]:

- (i) If $N_A < N_B$, the minority chains form slightly deformed random coils with both the average end height and its fluctuation proportional to $N_A^{1/2}$.
- (ii) If $N_A > N_B$; the minority chain adopts an inhomogeneous flowerlike conformation: the added chains

A form a stem of height H (containing N_B segments, behaving just like the brush chains of length N_B), whereas the remaining $N_A - N_B$ segments form a randomly coiled crown outside the brush. The stem is strongly stretched and fluctuates only weakly. The transition from adsorbed state to flower (or the reverse) occurs in a narrow range $N_B - N_A$, where the chains A are both strongly stretched and strongly fluctuating.

(iii) The case $N_A = N_B$ is trivial: the minority chain is identical to all other chains in the brush and adopts parabolic profile like all of the others.

The aim of the present paper is to investigate the properties of minority chains in regular polymer brushes. Such a two-component system may be referred to as a microheterogeneous brush. A small fraction of minority chains (length N_A) differs from the majority brush-forming chains (length N_B) not only in their length but in their chemical structure as well. The grafting density of the minority chains is assumed to be small enough to neglect the mutual overlap of these adsorbing chains. We consider further that $N_A > N_B$ so that for nonadsorbing A chains a flower conformation exists. However, A consists of adsorption-active monomers, and therefore the A chains are able to adsorb onto the grafting surface. Figure 1 gives a pictorial representation of an adsorbed conformation ($N_A < N_B$, left) and a flower conformation ($N_A > N_B$, right) in a brush of thickness H due to the B (brush) chains. A characteristic feature of the flower conformation (Figure 1, right) is the stretching of the stem part of the chain A to the same extent as the brush chains B. It is the competition between adsorption

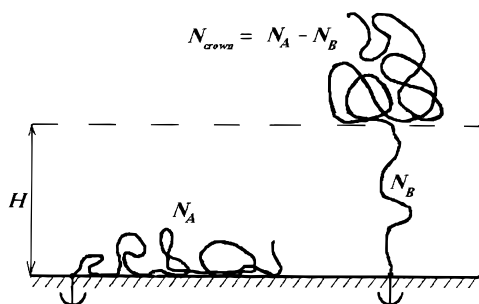


Figure 1. Schematic sketch of possible conformations of a minority chain in a polymeric brush. The minority long chain contains N_A segments; the brush chains have N_B segments. The broken line shows the brush thickness, H . Two different types of conformations for minority long chain are shown: the adsorbed state (left) and the flower state (right). In the latter case, the N_A segments split up in N_B segments in the stem and $N_{\text{crown}} = N_A - N_B$ crown segments.

(Figure 1, left) and stretching (Figure 1, right) that constitutes the central theme of our discussion.

The adsorption of an isolated polymer chain on a planar surface has been studied.^{3,9–11} A fundamental result of the adsorption theory is the existence of a threshold effect. If the energy of attraction ϵ of a chain segment is smaller than a certain critical value ϵ_{cr} , the macromolecule is not adsorbed. Hence, the parameter ϵ is considered to be positive for adsorption. If the energy ϵ is greater than the critical value ϵ_{cr} , the average number of contacts is proportional to the number of segments, and the average position of the chain end is independent of the chain length. For an asymptotically long chain, the critical energy is identified as a second-order transition point.^{9–11} Recently, the adsorption of a large assembly of chains, forming a brush, was examined for the case that each segment can adsorb onto the grafting surface.¹² As a result, the brush becomes spontaneously inhomogeneous: some of the chains are completely adsorbed on the surface, whereas the remainder constitute a regular brush.

We use two approaches, both known in the literature.^{1–4} The first one is a numerical mean-field model of a regular brush. In this case, there is no assumption made on the form of the potential profile $U(z)$ (z is the coordinate normal to the plane, which is situated at $z = 0$). From previous studies, it is known that the numerically found potential profile is approximately parabolic. The second approach is an analytical one. Here, we consider from the start a parabolic profile of the potential field, which is characteristic of strongly stretched brush chains. In both approaches, minority chains are introduced in the considerations.

Because the minority chain is fully surrounded by the excess of brush chains, the problem of finding the conformations of a minority chain in this brush is reduced to finding the chain conformation A in the external field $U(z)$. In this simplest case, the majority and the minority chains both experience the same potential profile $U(z)$. However, we assume that they still differ in their interaction with the grafting surface. This situation can be treated exactly in a lattice approach and allows a simplified analytical treatment as well.

We will show that the minority chains undergo a cooperative transition from an adsorbed state to a flower conformation with a stretched stem and a coiled crown. The end-point distribution of the minority chains turns

out to be bimodal around the transition point, which enables us to describe the conformational transition from an adsorbed chain to a flower conformation as a first-order phase transition (in the appropriate thermodynamic limit). Using a two-state approximation, we develop an analytical theory describing this chain-to-flower transition. The adsorption energy ϵ^* at the transition point depends only on the brush density and on the chain length ratio N_A/N_B of the adsorbing minority chains A and the brush chains B.

2. Mathematical Formulation

We consider the situation of long minority chains A added to a regular brush composed of shorter brush-forming chains B. The majority chains are composed of nonadsorbing segments. Both minority and majority chains are flexible (and of the same flexibility), the solvent is good for both A and B, and the A and B units mix athermally.

The grafting density of the minority chains is much less than $(N_A)^{-1}$, so we can neglect their mutual overlap. The minority chains A thus do not affect the density profiles formed by the majority chains B, and the problem is reduced to that of a single chain adsorbing in the presence of a constant external field (produced by the polymer brush).

Because we use both lattice and continuum models, we start with the mapping of both types of model, especially with respect to the adsorption interaction parameters (section 2.1). We also need to specify the form of the chemical potential field profile produced by polymer monolayer, and this will be discussed in section 2.2.

2.1. Adsorption of a Macromolecule in a Potential Field. There are two commonly used approaches to the mathematical description of polymer adsorption. The first one employs a lattice model,^{3,13} and the second one is based on a continuum description and uses a diffusion-type equation formalism.^{9,14,24} Both of these approaches are well-known and widely exploited.

2.1.1. Lattice Model. We consider a polymer chain lattice model characterized by a lattice parameter λ , which is the transition probability for a step from a given layer to an adjacent layer. In a simple cubic lattice, $\lambda = 1/6$. The bond length (lattice spacing) will be taken as unity. The lattice layers are numbered $z = 0, 1, \dots$, where $z = 0$ corresponds to the layer adjoining the surface. Hence, the grafted chains start in layer 0.

To account for segmental adsorption in such models, a short-ranged attractive potential is usually introduced acting on the chain in layer 0. An adsorption interaction parameter ϵ is defined as minus the free-energy change of a chain unit due to the formation of a contact between this unit and a surface. We express all of the energy parameters in units of kT . Adsorption corresponds to positive values of ϵ . An important characteristic, which depends on the lattice type, is the critical energy of adsorption

$$\epsilon_{\text{cr}} = -\ln(1 - \lambda) \quad (1)$$

Adsorption of a long chain in the absence of an external field starts when ϵ reaches the value ϵ_{cr} . For the simple cubic lattice (with $\lambda = 1/6$), $\epsilon_{\text{cr}} = \ln(6/5)$. Apart from this short-range adsorption interaction potential ϵ , an external field $U(z)$ may act on each of the chain

units. In the present paper, this external field is assumed to be produced by the brush-forming chains.

The statistical weight $P(z, n)$ for a chain having its n th unit in layer $z > 0$ from the surface obeys the well-known recurrence equation which was introduced by Rubin¹³ and generalized by others³ for various inhomogeneous polymer systems:

$$P(z, n+1) = \exp[-U(z)] [\lambda P(z-1, n) + (1-2\lambda)P(z, n) + \lambda P(z+1, n)] \quad (2)$$

The boundary condition which is equivalent to the recurrence equation for adsorbed segments (at $z = 0$) has the form:

$$P(0, n+1) = \exp[\epsilon - U(0)] [(1-2\lambda)P(0, n) + \lambda P(1, n)] \quad (3)$$

because $P(z, n)$ is zero for negative z . The initial condition corresponding to the chain grafting is represented by

$$\begin{aligned} P(0, 0) &= 1 \\ P(z, 0) &= 0 \quad \text{at } z > 0 \end{aligned} \quad (4)$$

which expresses that the first segment can only start from $z = 0$. Equations 2–4 can be solved numerically if the form of the $U(z)$ profile is known.

2.1.2 Continuum Model. In a continuum model, $P(z, n) dz$ can be identified with the statistical weight for a chain having its n th unit in the interval $(z, z + dz)$. According to Edwards,¹⁴ $P(z, n)$ satisfies the equation

$$\frac{\partial P}{\partial n} = \frac{1}{6} \frac{\partial^2 P}{\partial z^2} - U(z)P \quad (5)$$

The short-range interaction with the surface is introduced through the boundary condition¹¹

$$\left. \frac{\partial \ln P(z, n)}{\partial z} \right|_{z=0} = -c \quad (6)$$

while the initial condition is

$$P(z, 0) = \delta(z) \quad (7)$$

At $c > 0$, a macromolecule tends to stick to the surface; for $c < 0$, it is desorbed. The value $c = 0$ corresponds to the critical adsorption point. It has been shown^{10,15} that for isolated adsorbed chains $1/c$ corresponds to the average layer thickness.

2.1.3. Relation between the Adsorption Interaction Parameters in the Two Models. The above two models have proved to be fully equivalent in the description of polymer adsorption problems, not only for asymptotically long chains but also for chains of finite length.^{16,17} The mapping of the two adsorption interaction parameters, c and ϵ , was given earlier.¹⁶ For $\lambda = 1/6$, the parameter c can be written as

$$c^2 = -6 \ln[6q(-2 + \sqrt{3 + 1/q})] \quad \text{at } \epsilon \geq \epsilon_{cr} \text{ or } q \geq 1/6 \quad (8)$$

and

$$c = 6q - 1 \quad \text{at } \epsilon \leq \epsilon_{cr} \text{ or } q \leq 1/6 \quad (9)$$

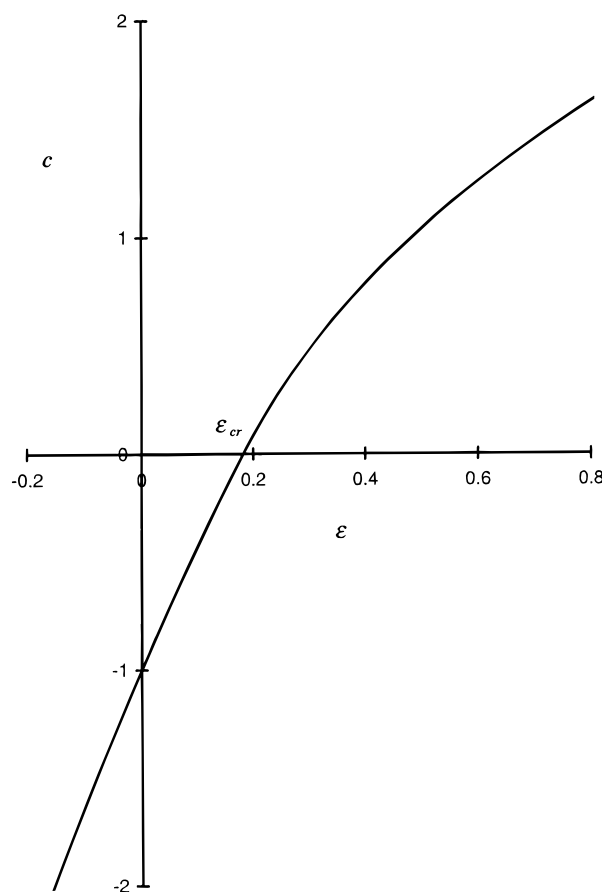


Figure 2. Relation between the adsorption interaction parameters c and ϵ as calculated by eq 8 for a 6-choice cubic lattice.

In these equations, q is defined as $q = 1 - \exp(-\epsilon)$, and $1 - \exp(-\epsilon_{cr}) = 1/6$.

There are asymptotic expansions of eqs 8 and 9 for both the strong and weak adsorption limits. At strong adsorption ($\epsilon \gg \epsilon_{cr}$), eq 8 reduces to

$$c^2/6 \approx \epsilon + \ln(4/6) \quad (10)$$

and the expansion at ϵ near ϵ_{cr} results in

$$c \approx 5(\epsilon - \epsilon_{cr}) - 65/6(\epsilon - \epsilon_{cr})^2 \quad (11)$$

Figure 2 displays the relationship between the parameters c and ϵ as given by eqs 8 and 9 for the case of a simple cubic lattice.

We shall use this relationship to compare the results obtained from the continuum and lattice models.

2.2. Potential Field Corresponding to a Regular Polymer Brush. The structure and properties of regular polymer brushes (i.e., homodisperse end-tethered chains, good solvents, and no adsorption energy) are well-investigated by now. The potential field in a brush is generated by the brush-forming chains only. It was shown before that in good solvents the self-consistent potential field $U(z)$ is related to the monomer density profile $\varphi(z)$ through

$$U(z) = -\ln[1 - \varphi(z)] \quad (12)$$

The field can be obtained either numerically by an iterative procedure or calculated analytically in the mean-field approximation.

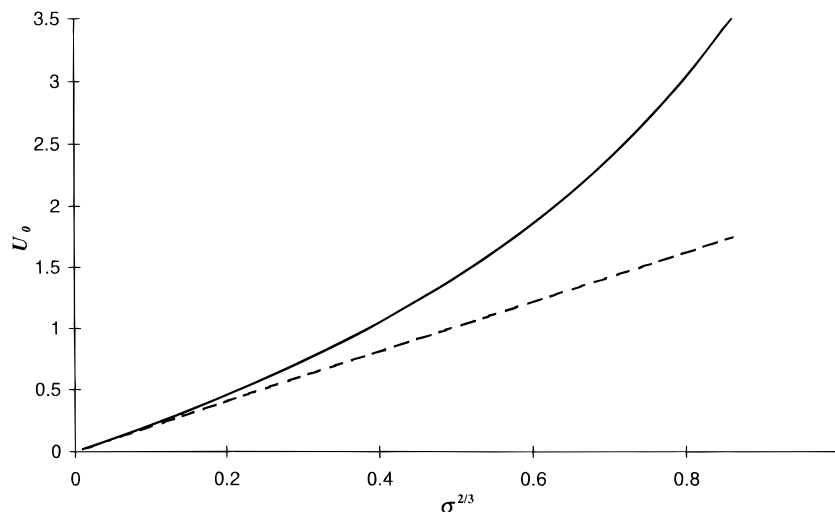


Figure 3. Parameter U_0 in eq 19 as a function of $\sigma^{2/3}$. The dashed line corresponds to the asymptotic eq 15.

The self-consistent-field numerical method was developed by Scheutjens and Fleer^{18,19} and used for studying the properties of regular polymer brushes.^{20,21} It is this standard SCF numerical procedure that we use in the present paper to calculate the field $U(z)$ corresponding to brushes of different chain length and grafting density.

It is well-known that at low grafting density both $\varphi(z)$ and $U(z)$ have a nearly parabolic profile^{19–22} and $\varphi(z) \approx U(z)$. The equilibrium properties of a monodisperse polymer brush of flexible chains are determined by the number of chain segments N_B , grafting density σ , and the solvent quality. According to Milner et al.,²² the analytical expression for $U(z)$ for a good solvent is

$$U(z) = U_0[1 - (z/H)^2] \quad (13)$$

Here, U_0 is the potential field at $z = 0$, and the brush height H is defined as the distance for which $U(z)$ becomes zero and is given, for not too high grafting density, by

$$H \approx (4\sigma/\pi^2)^{1/3} N_B \quad (14)$$

The parameter U_0 depends only on the grafting density σ . At low σ values, U_0 scales as

$$U_0 \approx \frac{3(\pi\sigma)^{2/3}}{2} \quad (15)$$

Analytical solutions for densely grafted brushes are also available.²³ The potential field $U(z)$ has an approximately parabolic profile even for densely grafted polymer layers. The more general equation, applicable also at high grafting densities, for the brush height H can be expressed in terms of U_0 and N_B as²³

$$H \approx \frac{2}{\pi} \sqrt{\frac{2U_0}{3}} N_B \quad (16)$$

and at dense grafting, U_0 is the root of the equation

$$\sqrt{U_0} - D(\sqrt{U_0}) = \pi\sqrt{\frac{3}{8}}\sigma \quad (17)$$

where $D(x)$ is the Dawson integral:

$$D(x) = \exp(-x^2) \int_0^x \exp(\tau^2) d\tau \quad (18)$$

The exact solution of eq 17 and the asymptotic one for low values of σ (eq 15) are shown in Figure 3. As follows from this figure, the asymptotic formula (15) is a reasonable approximation up to $\sigma^{2/3} \approx 0.2$ (i.e., to $\sigma \approx 0.06$). The same range of applicability can be assigned to formula (14).

Inserting eq 16 into eq 13 results in a general expression for the brush potential profile in terms of U_0 and N_B :

$$U(z) = U_0 - \frac{3\pi^2}{8} \left(\frac{z}{N_B} \right)^2 \quad (19)$$

which can be used for a wide range of grafting densities.

It was shown earlier²³ that eqs 19 and 17 are in an excellent agreement with the profiles obtained by the numerical SCF method. Small deviations near the wall and at the edge of the profiles exist and will be discussed below.

We have now formulated the problem both for the lattice and continuum models, defined all necessary parameters for both models and established the relations between these parameters. In our lattice calculations, we shall use ϵ as the adsorption interaction parameter and $U(z)$ profiles as obtained from the SCF method. The analytical theory is formulated in terms of the adsorption interaction parameter c , which is related to ϵ through eq 8. The function $U(z)$ is taken in the form of eq 19 at $z \leq H$ and $U(z) = 0$ at $z \geq H$, where U_0 is a known function of the grafting density σ (see eq 17 and Figure 3).

3. Numerical Results for a Long Minority Chain in a Brush

Prior to analyzing the behavior of minority chains, we show in Figure 4 some typical $U(z)$ brush profiles as obtained by the Scheutjens–Fleer SCF method³ for $N_B = 100$ and 400 and grafting density σ in the range from 0.02 to 0.3. As expected for small z , the field $U(z)$ does depend on only σ (approximately as $\sigma^{2/3}$), whereas the thickness H varies linearly with N_B and approximately linearly with $\sigma^{1/3}$. Clearly, the numerical model is in good accordance with analytical predictions. Fully in line with reports about this comparison in the litera-

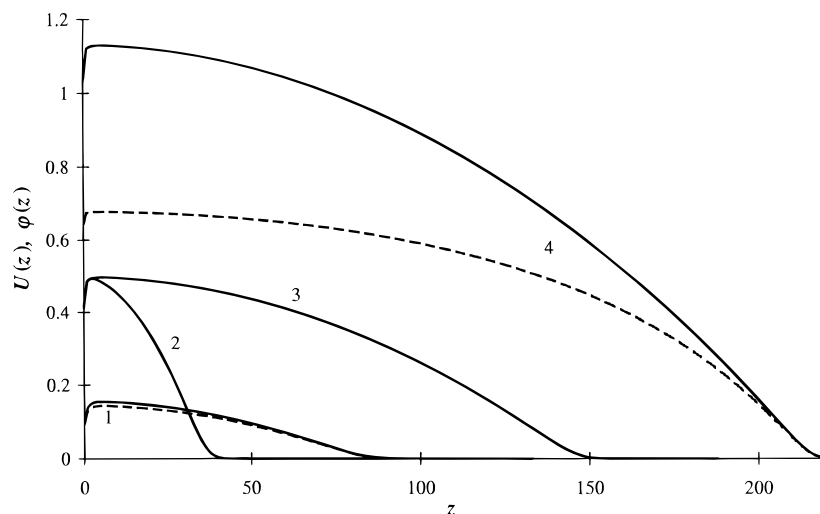


Figure 4. The potential field profiles $U(z)$ (solid lines) calculated by the numerical SCF method for polymer brushes of different density and chain length. $\sigma = 0.02$ (1), 0.1 (2 and 3), and 0.3 (4); $N_B = 100$ (2) and 400 (1, 3, and 4). In addition, the segment density $\varphi(z)$ (dashed lines) is shown for the lowest and highest grafting densities.

ture,¹⁹ we mention that at the outer edges of the profiles and near the surface there are features in the numerical data that are not covered by the analytical analysis. In particular, we stress the deviations near the surface. Near the surface, the numerical data indicate a drop of the segment potential, whereas the analytical model assumes that the profile remains parabolic all the way to the surface. The reason for the drop in density is that the chains of the brush cannot penetrate the surface. This leads to a loss in degrees of freedom for choosing chain conformations, and as a result, a depletion layer develops (both in densities and in segment potentials). Recall that $U(0)$ is the numerical segment potential in the surface layer and U_0 was used for the value expected from the analytical model, then $\Delta U_0 = U_0 - U(0)$ assumes a positive value. Two relevant comments can be made regarding the characteristics of the depletion zones. The first is that the relative importance of the discrepancy between analytical and numerical results $\Delta U_0/U_0$ decreases with increasing grafting density. The second is that at low grafting density the width of the depletion zone is larger than at higher grafting densities. The significance of both effects will be discussed below. We note that it is possible to (partially) mask these effects by introducing a weak adsorption energy for the brush chains (close to critical adsorption energy). We did not choose to do so, giving us the possibility to illustrate the effect of these nonuniversal features.

From the recurrence eqs 2–4, we obtained the chain end distribution functions $P(z, N_A)$ for the minority chains of length N_A in such brushes of length N_B . In all cases, $N_A > N_B$, and N_A was taken in the range of 100–2400 and the adsorption interaction energy ϵ of the minority chains was varied in the range $0 < \epsilon < 1.0$. We also calculated the average distance $\langle z \rangle$ of the free chain end from the adsorbing plane, its dispersion $\langle \delta z^2 \rangle = \langle z^2 \rangle - \langle z \rangle^2$, and the average fraction θ of adsorbed chain units. The latter quantity is defined as $\theta = \langle m \rangle / N_A$, where $\langle m \rangle$ is the number of contacts with the wall.

Figure 5 shows the $P(z, N_A)$ distribution functions for minority long chains with $N_A = 200$ in a brush with $N_B = 100$ and $\sigma = 0.1$, at several values of the adsorption energy ϵ [$P(z, N_A)$ is normalized in this figure]. For these distribution functions, the left-hand-side ordinate axis

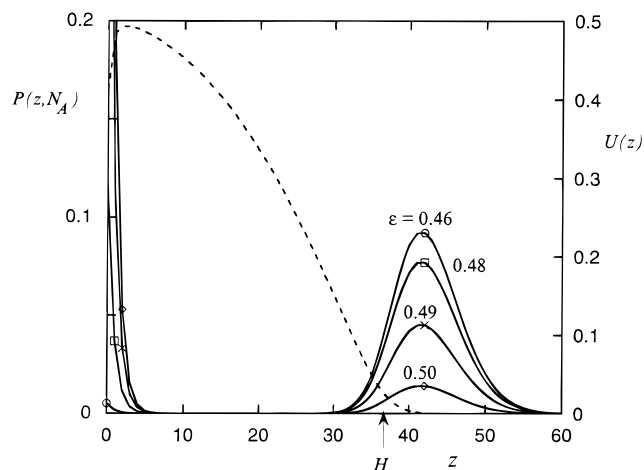


Figure 5. Distribution of the free end of minority long chains with $N_A = 200$ in a brush with $N_B = 100$ and $\sigma = 0.1$ at several values of the adsorption energy ϵ (left-hand-side ordinate axis). The potential field profile produced by the brush is shown by the dashed line and the arrow indicates the height H of the brush.

applies. The potential field profile $U(z)$ in the brush is shown by the dashed line (right-hand-side ordinate axis). The end height distribution turns out to be bimodal. One can clearly distinguish two states of a minority chain: the adsorbed state, localized near the grafting plane for relatively high ϵ , and a flower state, with a coil-like crown pushed outside the brush for low ϵ . For convenience, we have indicated the brush height $H \approx 36.6$ by an arrow. With increasing ϵ , the adsorbed state is more favorable, as expected. The range of ϵ in which the two states coexist [i.e., where the area under the $P(z, N_A)$ curve near the surface and near the brush edge is comparable] is rather narrow, and at constant ratio N_A/N_B , it tends to zero in the limit $N_A, N_B \rightarrow \infty$ (see the analysis below).

Figure 6 displays the average height of the free end $\langle z \rangle$ (Figure 6a), its dispersion $\langle \delta z^2 \rangle = \langle z^2 \rangle - \langle z \rangle^2$ (Figure 6b), and the average fraction of adsorbed segments θ (Figure 6c) as a function of the adsorption energy ϵ for minority chains of various lengths N_A . In this figure, the ratio of the minority chain length to that of a main chain was kept constant at $N_A/N_B = 2$ and $\sigma = 0.1$.

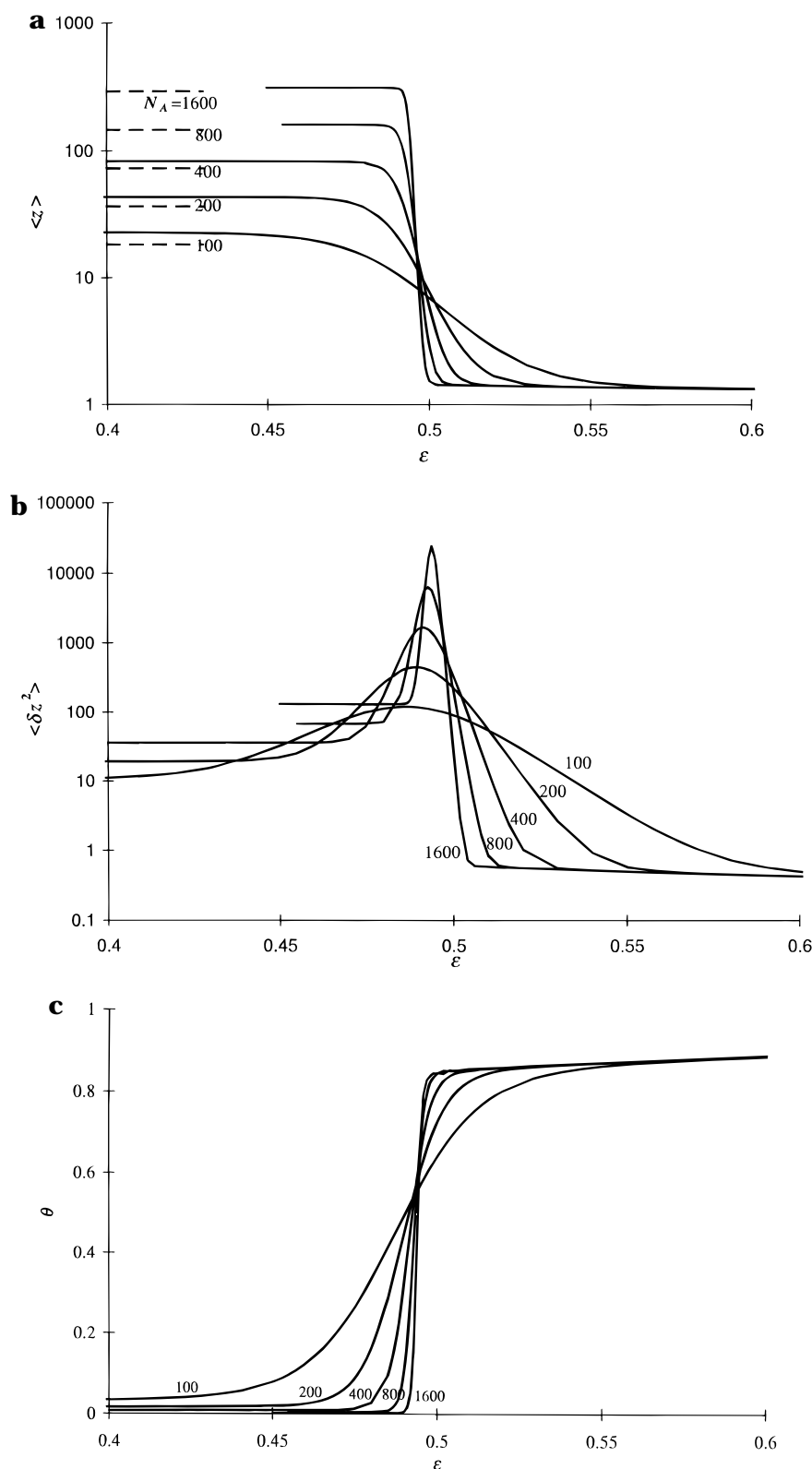


Figure 6. Dependences of (a) the average position $\langle z \rangle$ of the free end, (b) its dispersion $\langle \delta z^2 \rangle = \langle z^2 \rangle - \langle z \rangle^2$, and (c) the average fraction of adsorbed segments $\theta = \langle m \rangle / N_A$ for minority chains of different lengths N_A on the adsorption interaction parameter ϵ . The values of N_A are shown at the curves. The brush parameters are $\sigma = 0.1$ and $N_B = N_A/2$. The ordinate axes in a and b have logarithmic scales. In a, the brush height H is indicated as the dashed horizontal lines.

Figure 6a shows the flower state to the left (low ϵ) and the adsorbed state to the right (high ϵ). The brush thickness H is also indicated in the figure (dashed line). It can be seen that $\langle z \rangle$ for the flower state is somewhat higher than H . We return to this point in the analytical section. At large adsorption energy, not only the average

end height but also its fluctuations are small, as shown in Figure 6b. In this region, θ is on the order of unity (Figure 6c), as expected for a strongly adsorbing isolated minority chain. As ϵ decreases $\langle z \rangle$ increases rather abruptly, θ decreases steeply, and $\langle \delta z^2 \rangle$ passes through a maximum. Beyond that, at low ϵ , $\langle z \rangle$ and $\langle \delta z^2 \rangle$ become

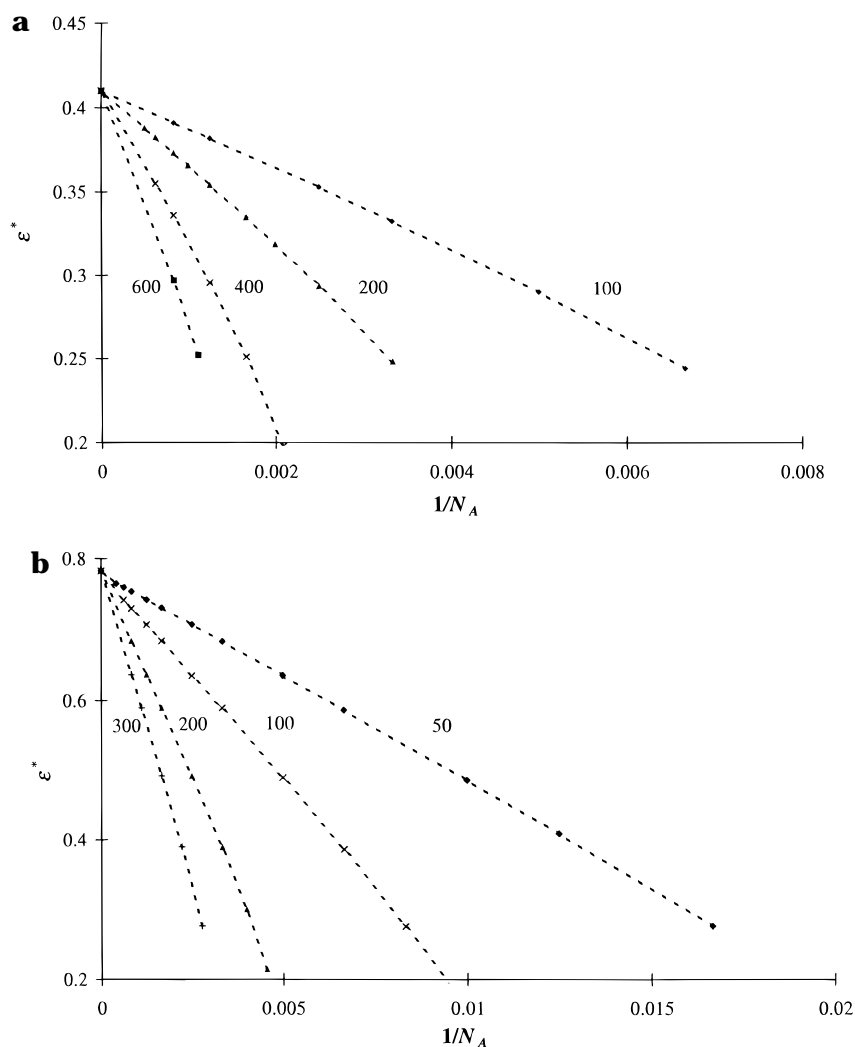


Figure 7. Dependencies of the transition-point energy ϵ^* upon $1/N_A$ for $\sigma =$ (a) 0.02 and (b) 0.1. The values of N_B are specified near the lines. The extrapolation of the numerical data toward $1/N_A = 0$ is shown as the dotted curves merging into one point on the ordinate axis.

essentially constant, at a level which increases with increasing N_A . At the same time, θ tends to zero. This is typical for a flower conformation of the minority chains.

Figure 6 shows that the transition between these conformations is rather smooth at small N_A . However, with increasing N_A (and $N_B = N_A/2$) the transition takes the form of a steplike function. Hence, we may define a transition-point energy ϵ^* which separates the two states. This may be determined from the intersection points in Figure 6a,c or from the position of the maximum in Figure 6b. For convenience, we choose the point where the dispersion $\langle \delta z^2 \rangle$ has its maximum.

Figure 7 displays the dependence of ϵ^* on $1/N_A$ at various N_B and grafting density $\sigma = 0.02$ (Figure 7a) and $\sigma = 0.1$ (Figure 7b). In all cases, ϵ^* is a decreasing function of $1/N_A$ which is almost linear. At given grafting density σ , all lines corresponding to different N_B values tend to the same limiting value, as shown by the extrapolation to $1/N_A = 0$ in Figure 7; these extrapolated curves (dotted) are drawn as a guide to the eye. The limiting value of $1/N_A = 0$ depends only on the grafting density σ .

Figure 8 displays the transition-point energy ϵ^* as a function of the ratio N_B/N_A for brushes of different grafting density. For each σ , N_B was varied in the range

from 50 to 600. As can be seen, every set of data corresponding to a given value of σ merges into a single line when plotted in the coordinates of Figure 8. All of the curves of Figure 7a collapse into the first line from below in Figure 8 ($\sigma = 0.02$) and those of Figure 7b into the second line from the top. In the following sections, we will discuss how all of the curves of Figure 8 may be transformed into one master curve by an appropriate scaling with σ .

To extract more physical insight from these numerical results, it is useful to develop an analytical treatment of the problem. This will be done in the next section.

4. Analytical Approach

A complete analytical solution of eqs. 5, 6, and 17 is still rather difficult. However the problem can be simplified by taking into account the bimodal character of the chain end distributions in the vicinity of the transition point: two types of minority conformations in a brush dominate. One is an adsorbed state in a nearly constant field $U(z) \approx U_0$, the other is a flowerlike conformation with a stem inside the brush and a coiled crown at the outside. The equations describing both types of conformations are available, so that approximate analytical equations for the problem under consideration can be easily constructed.

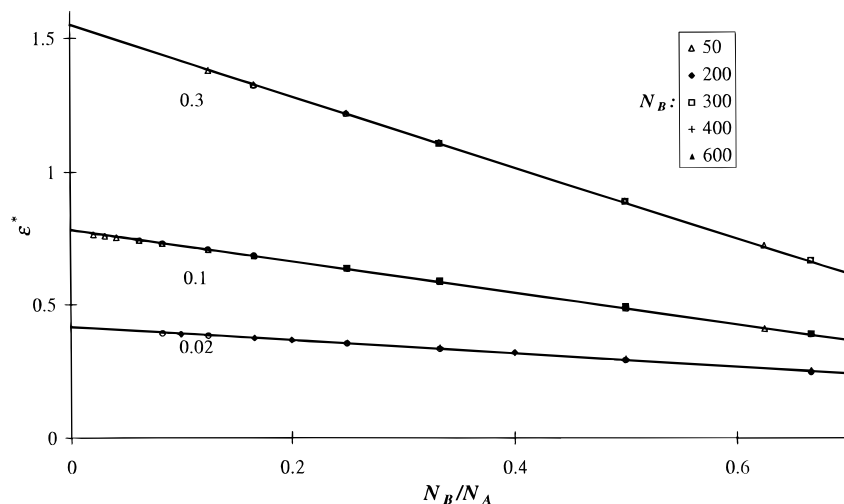


Figure 8. The transition-point adsorption energy ϵ^* as a function of the length ratio N_B/N_A . The values of N_B vary from 50 to 600. The grafting density σ is indicated.

4.1. Adsorbed State. A long polymer chain adsorbed inside a regular brush consists of trains and short loops. When the adsorption energy parameter ϵ is not very close to its critical value ϵ_{cr} , the length of a typical loop is independent of the molecular weight of the chain. We consider situations that the minority chains do not overlap. We assume that the main brush chains are long enough so that $n_{loop} \ll N_A$. Then, the effect of the potential profile $U(z)$ becomes trivial: it is the same as that of a constant potential U_0 . In this approximation, all of the restricted partition functions $P(z)$ for an adsorbed minority chain in the brush are given by those for an isolated adsorbed chain, $P_0(z)$, times the Boltzmann factor accounting for the constant external potential:

$$P(z) = P_0(z) \exp(-N_A U_0) \quad (20)$$

The solution of eqs 5 and 6 for an isolated Gaussian chain (fixed by one end on the plane) for which the segments can adsorb on the surface [i.e., for the case $U(z) = 0$] was obtained by Lepine and Caille²⁴ and others.⁹ This solution has the following form:

$$P_0(\tilde{z}) = (\pi R^2)^{-1/2} \{ \exp[-(\tilde{z})^2] [1 + \pi^{1/2} \tilde{c} Y(\tilde{z} - \tilde{c})] \} \quad (21)$$

where $R = (N_A/6)^{1/2}$ is the radius of gyration and the function $Y(t)$ is given by $Y(t) = \exp(t^2) \text{erfc}(t)$, with $\text{erfc}(t)$ the complementary error function. In eq 21, we introduced two scaled variables: $\tilde{z} = z/2R$ and $\tilde{c} = cR$. The function $Y(t)$ has the asymptotic behavior $Y(t) = 2 \exp(t^2)$ for $-t \gg 1$ and $Y(t) = 1 - (2/\sqrt{\pi})t$ for $|t| \ll 1$. Integrating over z gives the full partition function for a grafted isolated chain:

$$Q_0 = Y(-\tilde{c}) \quad (22)$$

According to earlier results,^{25,26} the restricted partition function for a chain with a given number m of adsorbed segments is

$$P_0(\tilde{m}) = (\pi R^2)^{-1/2} \exp(\tilde{c}^2) \exp[-(\tilde{m} - \tilde{c})^2] \quad (23)$$

where $m/2R$.

Using eqs 20–23, we obtain the following scaled averages for the minority chain in the adsorbed state: the number of contacts with the plane $\langle \tilde{m} \rangle$, the average

position of the free end $\langle \tilde{z} \rangle$, and the dispersion of the scaled height $\langle \delta \tilde{z}^2 \rangle$

$$\langle \tilde{m} \rangle = [\pi^{1/2} Y(-\tilde{c})]^{-1} + \tilde{c} \quad (24)$$

$$\langle \tilde{z} \rangle = [Y(-\tilde{c}) - 1] [2\tilde{c} Y(-\tilde{c})]^{-1} \quad (25)$$

$$\langle \delta \tilde{z}^2 \rangle = \left\{ \frac{[Y^2(-\tilde{c}) - 1]}{4} - \frac{\tilde{c} Y(-\tilde{c})}{\sqrt{\pi}} \right\} [\tilde{c} Y(-\tilde{c})]^{-2} \quad (26)$$

In the case of strong adsorption (at $\tilde{c} \gg 1$) the partition functions of a minority chain in an adsorbed state have the following asymptotic forms:

$$Q_{ads} \approx 2 \exp[(c^2/6 - U_0) N_A] \quad (27)$$

$$P_{ads}(z) \approx 2c \exp\left[\left(\frac{c^2}{6} - U_0\right) N_A\right] \exp(-cz) \quad (28)$$

$$P_{ads}(m) = (\pi R^2)^{-1/2} \exp[(c^2/6 - U_0) N_A] \exp\left[-\frac{3(m - c)^2}{2N_A}\right] \quad (29)$$

The average adsorbed chain parameters are now easily obtained:

$$\langle m \rangle_{ads} \approx 1/3 N_A c \quad (30a)$$

$$\langle z \rangle_{ads} \approx c^{-1} \quad (30b)$$

$$\langle \delta z^2 \rangle_{ads} \approx c^{-2} \quad (30c)$$

4.2. Flower Conformation of a Long Minority Chain. As shown in Figure 5, when $\epsilon < \epsilon^*$, a long chain in a brush with $N_A > N_B$ exists in a flowerlike conformation with a stretched stem and a coiled crown. Such conformations have been analyzed in detail,⁸ and the basic formulas for the flowerlike state are available. For deriving the partition function for the flowerlike state, we follow the lines of Skvortsov et al.⁸

The minimum of the mean-field free energy in the Newtonian strong-stretching limit corresponds to the conformation where the first N_B segments of the chain lie within the brush and the $N_{crown} = N_A - N_B$ remaining segments form a crown outside the brush. Then, the partition function for the flower conformation can be approximated as:

$$P_{\text{flower}}(z, N_A) \approx P_{\text{stem}}(N_B) P_{\text{crown}}(z, N_{\text{crown}}) \quad (31)$$

A nonexponential correction coming from integrating over all possible stem lengths is omitted in the present treatment.

The function P_{stem} in eq 31 has been calculated⁸ with the assumption that the stem part of the flower conformation can be considered as a chain in a brush with the N_B th segment fixed at brush height H . According to Skvortsov et al.,⁸ P_{stem} has the form:

$$P_{\text{stem}} \approx (3/N_B)^{1/2} \exp(-N_B U_0) \quad (32)$$

Because the flower conformation has a crown outside the brush (see Figure 5), it is reasonable to consider a crown as an isolated chain grafted to the outer brush boundary (i.e., to the repulsive planar surface that is situated at $z = H$). Note that the nonadsorbing boundary condition is practically equivalent to taking the limit of large negative c in the general boundary condition (6). It is well-known that the average number of segments contacting a repulsive plane is quite insensitive to the adsorption interaction strength, as long as it stays below a certain critical value. Therefore, the flower conformation can be approximated as being independent of c (or ϵ), and we can employ the results obtained for a nonadsorbing boundary condition. For $z > H$ we use eq 21 with large negative $\tilde{c} = cR_{\text{crown}}$, $\tilde{z} = (z - H)/(2R_{\text{crown}})$ and $R_{\text{crown}} = (N_{\text{crown}}/6)^{1/2}$. Then we have asymptotically for $N_{\text{crown}} \gg 1$

$$P_{\text{crown}}(z, N_{\text{crown}}) = \frac{1}{2\sqrt{\pi}R_{\text{crown}}^3} (z - H) \exp\left\{-\frac{(z - H)^2}{4R_{\text{crown}}^2}\right\} \quad (33)$$

For a polymer chain in the flower conformation, the restricted partition function for a given height of the free end is given by multiplying P_{stem} , eq 32, and P_{crown} , eq 33:

$$P_{\text{crown}}(z, N_A) \approx 9 \left(\frac{2}{\pi N_B}\right)^{1/2} \frac{(z - H)}{N_{\text{crown}}^{3/2}} \exp(-N_B U_0) \exp\left\{-\frac{3(z - H)^2}{2N_{\text{crown}}}\right\} \quad (34)$$

where $z > H$.

Integrating over z from H to infinity yields the partition function for the flower state:

$$Q_{\text{flower}} = \left(\frac{2}{\pi N_B}\right)^{1/2} \frac{3}{N_{\text{crown}}^{1/2}} \exp(-N_B U_0) \quad (35)$$

The average characteristics of flowerlike chains are

$$\langle z \rangle_{\text{flower}} \approx H + (\pi N_{\text{crown}}/6)^{1/2} \quad (36)$$

$$\langle z^2 \rangle_{\text{flower}} \approx H + (2\pi/3)^{1/2} H N_{\text{crown}}^{1/2} + {}^{2/3} N_{\text{crown}} \quad (37)$$

$$\langle \delta z^2 \rangle_{\text{flower}} \approx \frac{(4 - \pi)}{6} N_{\text{crown}} \quad (38)$$

The average number of contacts of a minority chain with the grafting surface is small, so $\langle m \rangle/N_A$ is close to zero.

4.3. Results of the Two-State Theory. As mentioned previously, we can write the partition function for a long minority chain in a brush as a sum over two

well-defined states:

$$Q = Q_{\text{ads}} + Q_{\text{flower}} \quad (39)$$

The average height of a free end is

$$\langle z \rangle = \langle z_{\text{ads}} \rangle \frac{Q_{\text{ads}}}{Q} + \langle z_{\text{flower}} \rangle \frac{Q_{\text{flower}}}{Q} \quad (40)$$

and similar expressions can be written for the other averages (e.g., the average number of contacts with the wall).

From eqs 27, 30, and 35–40, with $R_{\text{crown}} = \sqrt{(N_A - N_B)/6}$, we obtain the following asymptotic formulas for the flower state (F), the transition point (T), and the adsorbed state (A):

$$\frac{\langle m \rangle}{N_A} = \begin{cases} 0 & (F) \\ c/6 & (T) \\ c/3 & (A) \end{cases} \quad (41)$$

$$\langle z \rangle = \begin{cases} H + \sqrt{\pi} R_{\text{crown}} & (F) \\ {}^{1/2}(H + \sqrt{\pi} R_{\text{crown}}) & (T) \\ c^{-1} & (A) \end{cases} \quad (42)$$

$$\langle \delta z^2 \rangle \approx \begin{cases} (4 - \pi) R_{\text{crown}}^2 & (F) \\ \left(\frac{H}{2}\right)^2 \left[1 + 2\sqrt{\pi} \left(\frac{R_{\text{crown}}}{H}\right) + (8 - \pi) \left(\frac{R_{\text{crown}}}{H}\right)^2\right] & (T) \\ c^{-2} & (A) \end{cases} \quad (43)$$

The transition point is defined by the condition that the partition functions for the adsorbed and the flower states are equal. Retaining only the exponential terms in eqs 27 and 35, we get a surprisingly simple result for the transition point:

$$(c^*)^2/6 = U_0(1 - N_B/N_A) \quad (44)$$

We recall that U_0 is only a function of the grafting density; see eq 15 and 17 and Figure 3. Equation 44 describes the first-order transition line in the phase diagram. For $c^2 > 6U_0$, the adsorbed state is thermodynamically stable for minority chains of any length. In the opposite case, $c^2 < 6U_0$, minority chains with N_A less than the critical value

$$N_A^* = N_B(1 - c^2/6U_0)^{-1} \quad (45)$$

exist in the adsorbed state, whereas longer chains ($N_A > N_A^*$) take the flower conformations.

In the limit $N_A \gg N_B$, eq 45 reduces to $(c^*)^2 = 6U_0$ or (at $\sigma < 0.06$) to

$$c^* \approx 3(\pi\sigma/2)^{1/3} \quad (46)$$

The left-hand side of eq 46 can be interpreted as the inverse average thickness (the size of the adsorption blob) of an adsorbed isolated minority chain at the grafting plane. The right-hand side scales as the inverse blob size in the brush formed by majority chains. The condition for the free energies of the two states to be equal can thus be reformulated in terms of blob sizes. As soon as the adsorption blob size exceeds the blob size of the brush, the chain does not like to remain adsorbed.

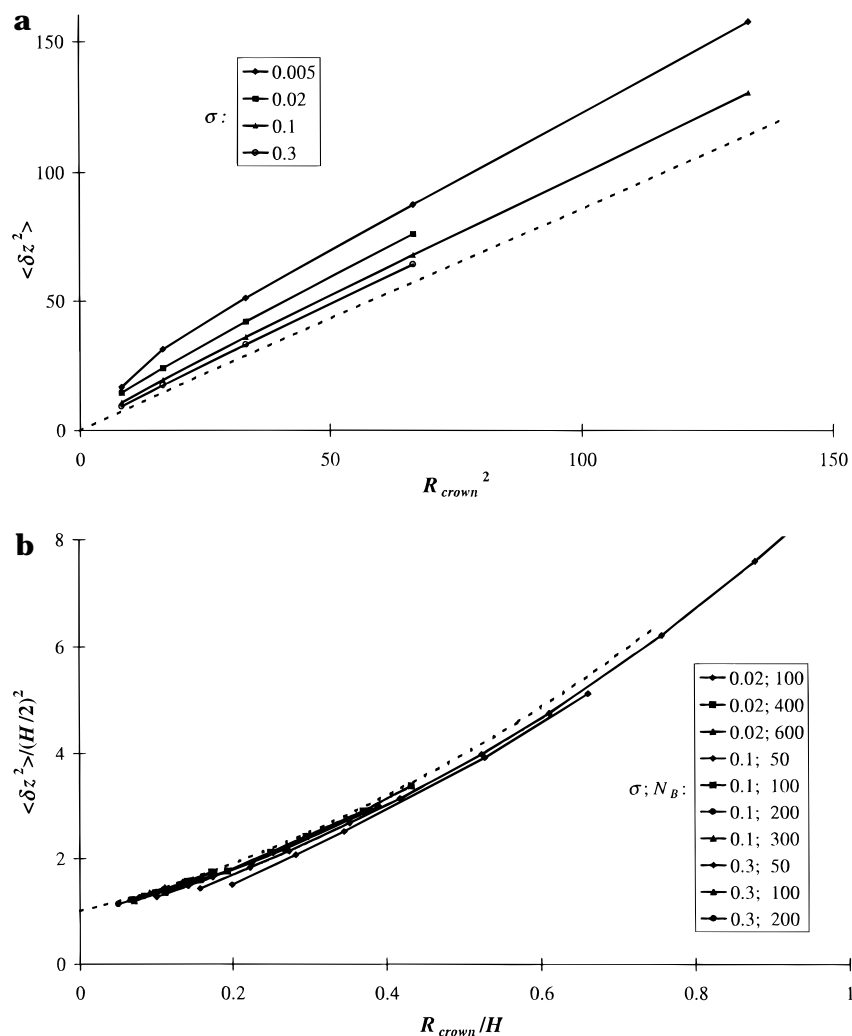


Figure 9. (a) Dispersion of the position of the free end of minority chains, $\langle \delta z^2 \rangle = \langle z^2 \rangle - \langle z \rangle^2$, as a function of R_{crown}^2 at an adsorption energy $\epsilon < \epsilon^*$ and (b) dependence of $\langle \delta z^2 \rangle / (H/2)^2$ on the ratio R_{crown}/H at the transition point $\epsilon = \epsilon^*$. The dotted lines are drawn according to eq 43.

Desorption in this case implies the formation of a flow-state as the chain remains terminally attached. If, on the other hand, the chains are not end-tethered, they may leave the brush as soon as the adsorption blob exceeds the brush blob, and they will be adsorbed otherwise. It is possible to measure experimentally the amount of adsorbed polymer by depletion experiments, and the affinity of the polymer for the surface can be altered by changing, for example, the temperature or some solution characteristic (adding displacers or changing the pH). Thus, one can measure the critical point of adsorption. Recall that the prediction of the transition point c^* indicates that this point is not a function of the molecular weight M_B of the brush chains, nor of that M_F of the free chains. The width of the adsorption/desorption transition is expected to be proportional to $(M_F)^{-1}$ (cf., Figure 6c). The transition point, eq 46, scales as the brush blob: it is a function of the brush grafting density only. As a consequence, one can deduce from an experimentally determined adsorption/desorption point for free chains the grafting density of the brush. This provides a new method to determine this quantity experimentally. As the adsorption/desorption transition of free chains adsorbing onto the grafting surface of the brush is a first-order phase transition, one should expect a peak in the heat capacity. These enthalpic effects can be measured by microcalorimetry. The origin of the heat

liberated at the transition is the sudden change in number of polymer-surface contacts and, therefore, the enthalpy of the transition scales as $M_F c^*$ per adsorbed molecule.

5. Comparison of Analytical and Numerical Results

According to eq 43 the dispersion $\langle \delta z^2 \rangle = \langle z^2 \rangle - \langle z \rangle^2$ of the free end in the flower state is approximately proportional to $R_{\text{crown}}^2 = (N_A - N_B)/6$, and it does not depend on the brush density σ . At the transition point the reduced dispersion $\langle \delta z^2 \rangle / (H/2)^2$ depends only on the ratio R_{crown}/H . In the adsorbed state, $\langle \delta z^2 \rangle$ depends neither on N_A nor on the brush parameters (see Figure 5).

Figure 9a displays the variation of the dispersion $\langle \delta z^2 \rangle$ as a function of R_{crown}^2 at $\epsilon = 0$ (flower regime) for minority chains of various length in brushes of various density. Figure 9b shows the dependence of $\langle \delta z^2 \rangle / (H/2)^2$ at the transition point on the parameter R_{crown}/H . One can see that in both cases the agreement between numerical and analytical results is quite reasonable. Upon an increase of grafting density σ , the curves found by the numerical method in Figure 9a tend toward the dotted straight line. The slope of this line is $(4 - \pi) \approx 0.86$, which corresponds to part F of eq 43. In Figure

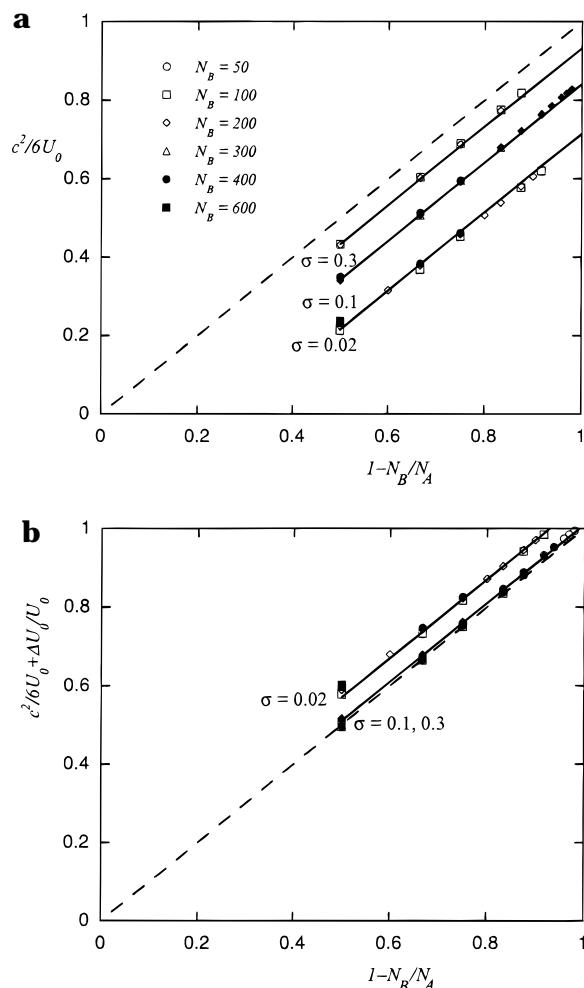


Figure 10. (a) Phase diagram of a long minority chain in a polymer brush in the coordinates $c^2/6U_0$ versus $(1 - N_B/N_A)$. Points represent the numerical data shown in Figure 8. The dashed line is the prediction of eq 44. The solid lines are guides for the eye “connecting” data points for the indicated grafting densities. (b) Phase diagram of a long minority chain in a polymer brush in the coordinates $c^2/6U_0 + \Delta U/U_0$ versus $(1 - N_B/N_A)$.

9b, all of the numerical data points, corresponding to different values of σ , N_B , and N_A values, are situated very closely to the dotted curve expressing the analytical result of part T of eq 43.

Let us return for a moment to Figure 8, which shows the transition-point energy ϵ^* as a function of the ratio N_B/N_A at several values of the grafting density σ , and try to find a master curve representing the phase diagram of our system. According to eq 44, we should replot the data for various values of N_A , N_B , and σ in the coordinates $(\epsilon^*)^2/6U_0$ versus $(1 - N_B/N_A)$. This is done in Figure 10a. It is clear that not all of the data collapse onto a universal line as suggested by eq. 44. Instead we see systematic deviations as a function of the grafting density. One may suggest that the origin of the failure is the fact that in the numerical calculations a real brush profile with a self-consistent value of $U(0)$ near the wall was used whereas in the analytical predictions a constant U_0 value was taken. It was concluded from Figure 4 that the relative difference between $U(0)$ and U_0 increases with decreasing grafting density. The deviations seen in Figure 10a are of the same order. To test this hypothesis, we have replotted in Figure 10b the same data, taking into account the

difference in external field potential for the adsorbing state in layer $z = 0$. The conclusion from this operation is indeed that the lines tend to the master curve for high grafting densities, but for low grafting densities some overcompensation occurs. This overcompensation can easily be explained. We recall that at low grafting densities the width of the depletion region near the surface is wider than for high grafting densities. This means that $U(1)$ [and perhaps $U(2)$] also deviates from U_0 . Moreover, the adsorption energy, ϵ^* , at the transition for low brush grafting densities is lower than for high brush grafting densities. The layer thickness is proportional to ϵ^{-1} , and thus, we should expect an adsorbed layer with more loops. These loops can probe the potential $U(1)$, which is between $U(0)$ and U_0 . In the compensation, it was wrongly assumed that all adsorbed segments were feeling $U(0)$, but some of them feel $U(1)$. Consequently, an overcompensation is produced. Recall again, that when for the brush-forming chains a weak adsorption energy (close to critical) would have been used, the depletion dip near the surface would have been nearly absent and all points would have collapsed onto the dashed line in the coordinates of Figure 10a. Thus, when nonuniversal features near the surface are absent, we may expect that the analytical predictions correctly give the phase diagram of the system. Therefore in the following we will discuss the feature of the phase diagram concentrating on the dashed line (predicted from eq 44).

Figure 10 can be viewed as the phase diagram for an adsorption transition of a long minority chain in a polymer brush. The values of the adsorption interaction parameter, the brush density, and the contour length ratio N_B/N_A that fall above the dashed line result in adsorbed minority chains localized near the grafting plane; the parameter combinations below the line produce a flower conformation.

It is clear from the phase diagram of Figure 10 that, by changing the adsorption interaction parameter for minority chains, one can cross the line and a conformational transition will occur. This transition is accompanied by a jump in the position of the free end and in the number of contacts with the plane (see Figure 6a,c) and therefore by an enthalpy jump. In the thermodynamic limit $N_A \rightarrow \infty$, $N_B \rightarrow \infty$, one can expect the transition to become a first-order phase transition.

At constant adsorption interaction, a conformational transition can be achieved by changing the brush density σ or the contour length ratio N_B/N_A .

6. Discussion

When a minority chain (with length N_A) which is able to adsorb onto a grafting planar surface is placed in a monodisperse brush (composed of nonadsorbing chains of length N_B), it can take one of two types of conformation: adsorbed or flower (provided that $N_A > N_B$). The adsorption strength at which the transition occurs depends on the grafting density of the brush-forming chains and on the chain length ratio. The transition between these two conformations has features of a first-order phase transition with an abrupt change in the energy and in the average position of the chain free end.

When $N_A < N_B$, the situation is of minor interest. The adsorption transition from an adsorbed state to a mushroom inside the brush will only differ slightly from the adsorption transition in absence of a brush. This transition is known to be a second-order transition.

When the minority chain length approaches the length of the main chain $N_A \rightarrow N_B$, the transition point tends to $c = 0$ as in the case of $N_A < N_B$, but now the transition is from an adsorbed state to a stretched one resembling the conformations of the brush chains. In this case, the distinct flower state cannot develop, and as a consequence, a continuous second-order transition is again expected. Thus, only when $N_A > N_B$ is the transition first-order. The case $N_A \approx N_B$ is rather delicate, and a detailed analysis of this situation will be presented in a separate paper.

Because minority chains in the adsorbed state are surrounded by brush-forming chains, one might be tempted to draw an analogy with the adsorption of polymers from a semidilute solution. However, the situation becomes qualitatively different when the minority chain is long enough to explore the space outside the brush. Then the situation resembles that of an isolated polymer chain adsorbing onto a plane in the presence of a finite-range repulsive external field. In good approximation, this field can be considered as constant in the region close to the grafting plane as follows from the following arguments.

From eq 27, it follows that the free energy per segment for a minority chain in the adsorbed state is a parabolic function of the adsorption parameter c :

$$N_A^{-1}F_{\text{ads}}(c, U_0) \approx U_0 - c^2/6 \quad (47)$$

In the previous section, we proved that for densely grafted brushes the detailed structure of the brush is not very important.

At the same time, the free energy of the flower conformation is independent of c :

$$N_A^{-1}F_{\text{flower}} \approx \frac{N_B}{N_A}U_0 \quad (48)$$

Thus, the flower conformation is also rather insensitive to the structure of the brush, as long as the brush provides an effective repulsive plane for the crown of the flower to develop. The two branches of the free energy (a parabola, eq 47, and a straight line, eq 48) are limiting equations for long minority chains (as well as long brush chains), and the intersection of these two branches corresponds to a first-order phase transition. As for densely grafted brushes, both branches do not depend strongly on the detailed structure of brush, and we thus can consider a step-function for the repulsive external field $U(z)$ without losing the characteristics of the transition. In principle, similar phenomena may thus be expected for end-grafted adsorbing chains in arbitrary external steplike potential profiles.

Microheterogeneous polymer brushes present a class of systems with remarkable properties. As in our system, we have shown that small changes in external conditions or changes in chain length ratio can influence the structural properties of the minority component dramatically. The minority chain can either be on the outside of the brush or hidden away on the inside. This may have significant consequence with respect to, for example, adhesion effects in colloidal stability or cell recognition in biological systems. It is very likely that it will prove possible to design applications which are adaptive in the sense that some surface property can

be switched on or switched off by the mechanism discussed above. For such a system to be of practical interest, however, it is necessary that the time scale needed for the switching is fast enough for the response time needed in the application. Thus, the investigation of the dynamics of such heterogeneous brushes is of special interest.

Many further extensions and generalizations of the present analysis are of considerable interest as well. For example, one may study the influence of the grafting density of minority chains and the effect of differences in solvent quality of the two types of chains. Work along these lines is in progress.

Acknowledgment. This work was supported in part from the program "Polymer Physics in Food Systems" financed by the Dutch Research Organization (NWO). A.M.S. and A.A.G. are thankful to Dr. Leonid Klushin for a helpful discussion on the flower conformations of macromolecules. A.M.S. is grateful to the Russian Foundation for Basic Research for financial support (Grant RFBR 97-03-322661a).

References and Notes

- (1) Milner, S. T. *Science* **1991**, *251*, 905.
- (2) Halperin, A.; Tirrell, M.; Lodge, T. P. *Adv. Polym. Sci.* **1991**, *100*, 31.
- (3) Fleer, G. J.; Cohen Stuart, M. A.; Scheutjens, J. M. H. M.; Cosgrove, T.; Vincent, B. *Polymers at Interfaces*; Chapman and Hall: London, 1993.
- (4) Zhulina, E. B.; Borisov, O. V.; Priamitsyn, V. A. *J. Colloid Interface Sci.* **1990**, *137*, 495.
- (5) Kent, M. S.; Lee, L. T.; Factor, B. J.; Rondelez, B. J.; Smith, G. S. *J. Chem. Phys.* **1995**, *103*, 2320.
- (6) Auroy, P.; Auvray, L.; Leger, L. *Macromolecules* **1991**, *24*, 2513.
- (7) Klushin, L. I.; Skvortsov, A. M. *Macromolecules* **1991**, *24*, 1549.
- (8) Skvortsov, A. M.; Klushin, L. I.; Gorbunov, A. A. *Macromolecules* **1997**, *30*, 1818.
- (9) Eisenriegler, E.; Kremer, K.; Binder, K. *J. Chem. Phys.* **1982**, *77*, 6296.
- (10) Gorbunov, A. A.; Skvortsov, A. M. *Adv. Colloid Interface Sci.* **1995**, *62*, 31.
- (11) De Gennes, P. G. *Rep. Prog. Phys.* **1969**, *32*, 187.
- (12) Currie, E. P. K.; Leermakers, F. A. M.; Cohen Stuart, M. A.; Fleer, G. J. *Macromolecules* **1999**, *32*, 487.
- (13) Rubin, R. J. *J. Chem. Phys.* **1965**, *43*, 2392.
- (14) Edwards, S. F. *Proc. Phys. Soc., London* **1965**, *85*, 613.
- (15) Gorbunov, A. A.; Skvortsov, A. M. *Vysokomol. Soedin., Seria A* **1986**, *28*, 2170.
- (16) Gorbunov, A. A.; Skvortsov, A. M. *Vysokomol. Soedin., Seria A* **1989**, *31*, 1244.
- (17) Fleer, G. J.; van Male, J.; Johner, A. *Macromolecules* **1999**, *32*, 825, 845.
- (18) Cosgrove, T.; Heath, T.; Van Lent, B.; Leermakers, F. A. M.; Scheutjens, J. M. H. M. *Macromolecules* **1987**, *20*, 1692.
- (19) Wijmans, C. M.; Scheutjens, J. M. H. M.; Zhulina, E. B. *Macromolecules* **1992**, *25*, 2657.
- (20) Hirtz, S. J. Modeling of Interactions between Adsorbed Block Copolymer. M.Sc. Thesis, University of Minnesota, Minneapolis, MN, 1988.
- (21) Skvortsov, A. M.; Pavlushkov, I. V.; Gorbunov, A. A. *Vysokomol. Soedin., Seria A* **1988**, *30*, 453.
- (22) Milner, S.; Witten, T.; Cates, M. *Macromolecules* **1988**, *21*, 2610.
- (23) Skvortsov, A. M.; Pavlushkov, I. V.; Gorbunov, A. A.; Zhulina, E. B.; Borisov, O. V.; Priamitsyn, V. A. *Polym. Sci. USSR* **1988**, *30*, 1706.
- (24) Lepine, Y.; Caille, A. *Can. J. Phys.* **1978**, *56*, 403.
- (25) Skvortsov, A. M.; Gorbunov, A. A.; Klushin, L. I. *J. Chem. Phys.* **1994**, *100*, 2325.
- (26) Gorbunov, A. A.; Skvortsov, A. M. *J. Chem. Phys.* **1993**, *98*, 5961.